



Deposited via The University of Leeds.

White Rose Research Online URL for this paper:

<https://eprints.whiterose.ac.uk/id/eprint/140645/>

Version: Accepted Version

Article:

Yao, G, Zhao, J, Ramiseti, SB et al. (2018) Atomistic Molecular Dynamic Simulation of Dilute Poly(acrylic acid) Solution: Effects of Simulation Size Sensitivity and Ionic Strength. *Industrial and Engineering Chemistry Research*, 57 (50). pp. 17129-17141. ISSN: 0888-5885

<https://doi.org/10.1021/acs.iecr.8b03549>

© 2018 American Chemical Society. This document is the unedited Author's version of a Submitted Work that was subsequently accepted for publication in *I&EC Research* after peer review. To access the final edited and published work see; <http://doi.org/10.1021/acs.iecr.8b03549>

Reuse

Items deposited in White Rose Research Online are protected by copyright, with all rights reserved unless indicated otherwise. They may be downloaded and/or printed for private study, or other acts as permitted by national copyright laws. The publisher or other rights holders may allow further reproduction and re-use of the full text version. This is indicated by the licence information on the White Rose Research Online record for the item.

Takedown

If you consider content in White Rose Research Online to be in breach of UK law, please notify us by emailing eprints@whiterose.ac.uk including the URL of the record and the reason for the withdrawal request.

Atomistic molecular dynamic simulation of dilute polyacrylic acid solution: effects of simulation size sensitivity and ionic strength

Guice Yao¹, Jin Zhao¹, Srinivasa B. Ramiseti¹, Dongsheng Wen^{2, 1}*

¹School of Chemical and Process Engineering, University of Leeds, Leeds, LS2 9JT, UK

²School of Aeronautic Science and Engineering, Beihang University, Beijing, 100191, P. R.

ABSTRACT

Physical properties of polyelectrolytes have been shown to be significantly related to their chain conformations. Atomistic simulation has been used as an effective method for studying polymer chain structures, but few has focused on the effects of chain length and tacticity in the presence of monovalent salts. This paper investigated the microscopic conformation behaviours of polyacrylic acid (PAA) with different chain sizes, tacticity and sodium chloride concentrations. The hydrogen behaviours and corresponding radial distribution functions were obtained. The results showed that the increase of salt concentrations led to the collapse of PAA chains, especially for longer chains. It was found that the effects of salt were mainly attributed to the shielding screening effect by sodium ions rather than the hydrogen bonding effect. Two different structure were form by iso-PAA and syn-PAA, respectively, which due to the deprotonation patterns along the PAA chain.

Key words: Molecular dynamics simulation, poly (acrylic acid), polymer conformation, salinity effect, tacticity

1. Introduction

Polyacrylic acid (PAA) as a water solvable macromolecular is widely used in industrial applications such as pigments in paint ¹, additives in coating and pH responsible materials in drug delivery ²⁻⁴. In particular, due to the water absorbing properties, PAA is applied as a thickening and suspension agent for petroleum recovery. The additives of PAA increase the viscosity of aqueous phase to reduce the mobility ratio during an enhanced oil recovery (EOR) process ⁵. This viscosification relies on the high-molecular weight ^{6, 7}, the degree of neutralization ⁸, and the environmental situations such as salinity ⁹ and pH values ¹⁰. Three main theories have been proposed in explaining polymer viscometric behaviours: electrical Theory ¹¹, folding-chain Theory ¹² and swarm Theory ¹³, and all of them indicate that the polymer configuration affects greatly its physical properties such as viscosity and wettability.

The polymer chain expansion occurs as monitored by increasing specific viscosity and radius of gyration and decreasing sedimentation and translational diffusion coefficients ^{14, 15}. To obtain information about the conformation of polyelectrolytes in aqueous solution and consequently to reveal the mechanism of its physical properties, a series of studies have been performed by different experimental techniques. The shrinkage and swelling phenomenon of PAA chains were evaluated successfully by using quartz crystal microbalance with dissipation monitoring (QCM-D) ¹⁶. The fluorescence label method was employed to monitor

PAA chains conformation at the alumina-water interface. An increase of polymer concentration was found to stretch polymer chains^{17,18}. The conformation transition of PAA chains as a function of ionic strength was determined by adsorption isotherms and force measurements using atomic force microscopy (AFM). As ionic strength increases, the repulsive force between the negatively charged carboxylate groups along the PAA chain was reduced due to the counter-ion screening, leading to the change of PAA conformation from a stretched to a coiled configuration¹⁹. The deuteron magnetic resonance (DMR) spectra titration was used to study the conformation in protein and weakly charged polyelectrolytes^{20,21}.

In addition, the dynamic light scattering (DLS) measurements, supplemented by static light scattering (SLS) and more advanced small-angle neutron scattering (SANS) methods, are widely adopted to study the chain conformation of polyelectrolytes, such as PAA, poly(styrenesulfonate) (PSS), and PMA²²⁻²⁸. Based on the presented investigations, the changes of polymer conformation are mainly attributed to the following parameters: charge density of backbone, counter-ion screening effect, special counter-ion bonding effect, and solvate quality. It should be addressed that these four factors are interacted each other as well. The ionization of polymer always related to the solubility, which in return, makes the solvate is regarded as good solvate or poor solvate^{25,26}. The poor solvent conditions give rise to a competition between the attractive interaction of the backbone and the electrostatic repulsion of polyelectrolytes charges. Adding organic solvents into dilute polyelectrolytes solutions, a counter-ion specific coil-globule transition occurs, which is not solely driven by the solvent quality, but also related to counter-ion binding and temperature as well^{29,30}. Besides, with addition of salts into solutions^{24,31}, the shielding effect strengthens as well as the solvate quality decrease. Therefore, the PAA molecules gradually collapse due to the counter-ion screening effect. For monovalent sodium chloride, continually dissolving salt into solutions, a so called theta solvent condition reached, where the PAA molecules stay an unperturbed conformation^{32,33}. The chain expansion due to a decrease in the concentration of salt could be satisfactorily interpreted by a theory by Peterlin et al.³⁴ and a worm like chain model applied by Kratky et al.³⁵. When the amount of salt concentration exceeds a specific value, the precipitation of polyelectrolytes with salt, usually called “salting out” occurs³⁶. In contract, if the multivalent salt ions are adopted, the polyions are binding with cations and consequently forms a further globule coil^{25,26,37}. This transition depends on the types, concentrations and even size of cations²⁹. These behaviours have been captured in the field-theoretical studies^{38,39}, which succeed in achieving a qualitative understanding of strong polyelectrolyte behaviour. However, they don't have the capacity for chemical detailed description and they do not provide a molecular-level insight on the morphology of polymer chains. In addition, some physical interactions vary form polymer chemical structure. The effect of tactility and the characteristic of hydrogen-bonding effect is normally difficult to interpret or require prior knowledge, which are not easily accessible to be achieved experimentally in advance.

Molecular dynamics (MD) simulation, on the other hand, has proven to be a valuable tool to study the self-assembly of polymers at the microscopic level, which could reveal detailed three dimensional conformational and structural behaviour⁴⁰⁻⁴³. The physical structure and thermodynamics properties of NaCl in water have been abundantly investigated in prior investigations using both experimental and numerical methods⁴⁴⁻⁵¹. For long-chained PAA, Reith et al⁵² adopted a coarse-grained model and the results were supported by DLS data.

Several other coarse-graining strategies were also employed to study the size and pH effects⁵³⁻⁵⁵, the influences of salt cations⁵⁶ and even the effect of solvent quality⁵⁷⁻⁵⁹ on conformation behaviours of polymer chains. However, the coarse-grained model failed to capture the hydrogen bonding effects, interactions between charged ions⁶⁰ and the effects of tacticity⁶¹. The solvent quality was studied just by changing the interaction parameters between the polymer and solvent, which cannot tell a real interaction for a specific solvent and cannot tell whether a solvent is in good or poor quality for a certain polymer. To reveal these effects, Sulatha et al adopted atomistic MD simulation method with Gromos 53a6 force field and showed that the radius of gyration of a single PAA was dependent on the charge density along the chain. The corresponding hydrogen behaviours and counter-ions distribution can be well captured by MD simulations^{62, 63}. Similar force field was used to study the conformation behaviours of PAA chains with different concentration or non-water-solvate conditions^{64, 65}, as well as the effect of salt species⁶⁶. It was found that there was a strong binding between divalent $\text{Ca}^{2+}/\text{Al}^{3+}$ and polyion, which led to Na^+ far away from the PAA chain⁶⁷⁻⁶⁹. The atomistic molecular dynamics simulation was also achieved to characterise the effect of tactics on polymer conformations in salt free solutions both in single or multi-chain system^{65, 70}. Different associations attributed to tacticity and deprotonation are indeed influence the polymer behaviours in salt free solutions.

It shall be noted that there were a wide variation of the number of monomers of PAA chains (i.e., chain size) and solvent molecules used in different studies, which could lead to different results^{60, 71}. A systemic study about this simulation size sensitivity, in the presence of different salts, to reveal the details of a single PAA chain has not been studied, which forms the motivation of this work. Besides, so far, few studies consider the effect of tacticity in salt solutions. Whether the different initial configurations behave different in the presence of salt and the detailed mechanism have not been revealed. Even for the salt free solutions, the effect of tacticity has not been fully understood from molecular level especially for weak polyelectrolytes. In this study, a series of PAA chains with different numbers of monomers and tacticity, which are functions of degrees of ionization (DoI) and salinity, were applied. The radius of gyration, species radial distribution functions and hydrogen effects were calculated and analysed in each system to reveal the atomic level mechanism of the PAA conformational behaviour, as detailed below.

2. Computational details and validations

2.1 Model

Six different numbers of monomers (i.e., 20, 30, 40, 50, 80, and 100 respectively) of isostatic PAA chains were generated using Bernoullian statics by assigning random dihedral angle values. Six values of DoI (i.e., 0, 0.2, 0.4, 0.6, 0.8, and 1.0, respectively) for each polymer chain were achieved by random deprotonation of the carboxylic acid groups along the chain. For 20 monomers PAA, another two different polymer chains with different tacticity but same deprotonation and DoI were built as well, detailed information is shown in **Table S1-S3** in supporting documents. The DoI, f , was defined as the ratio between the number of charged monomers, N_c , and the total number of monomers along the chain, N_m . Appropriate numbers of water molecules were put into cubic boxes to keep the PAA concentration approximately the same in all the cases. For $N_m=20, 30, 40,$ and 50 , 4000, 6000, 8000 and 10000 water molecules, respectively, were included in simulation box, which led to PAA concentration of

approximately 1.96 wt%. The Na⁺ counter-ions were added into simulation boxes for the neutrality of the system. In addition, the effects of solvent volume were also conducted for 50-monomers-PAA solutions by increasing the number of water molecules to 78800 (i.e., box length of 13.4 nm). **Figure 1(a)** showed the front view of the simulation box containing 20-monomers-PAA, water molecules and Na⁺ ions. An extended conformation was allocated as an initial structure of the PAA chain.

The salt ionic strength was adjusted by adding additional Na⁺ cations and Cl⁻ anions into the solvated box. The values of salt concentration were varied from 0.01 M to 1.4 M for 20-monomers PAA solutions, and from 0.1 M to 0.85M for 30-monomers PAA solutions, respectively. An example of a 20-monomers-PAA solution with 0.33 M NaCl was shown in **Figure 1 (b)**.

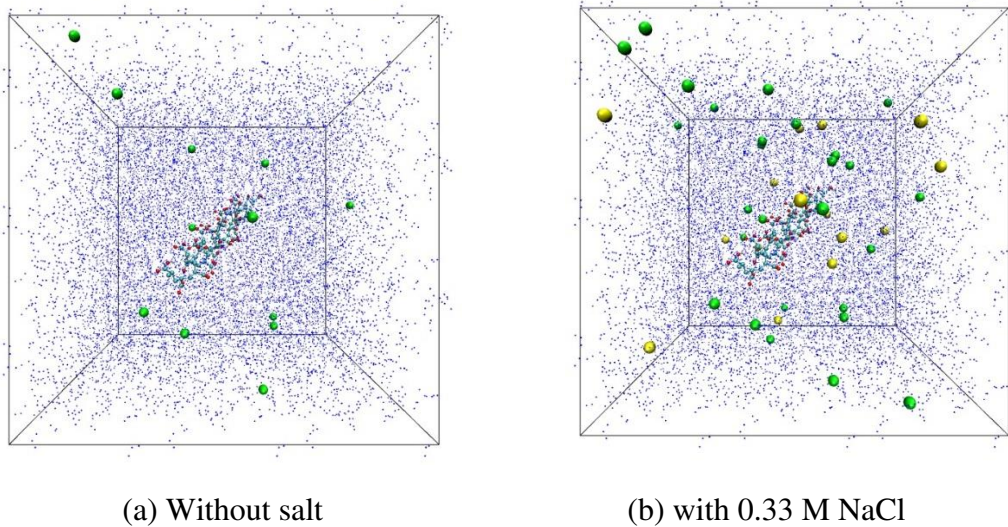


Figure 1 The initial configuration of the 20-monomers-PAA solution with $f=0.4$ (blue: water; red and white: oxygen and hydrogen atoms along the PAA chain, respectively; cyan: PAA backbone; green and yellow: Na⁺ and Cl⁻ ions)

2.2 Potential parameters

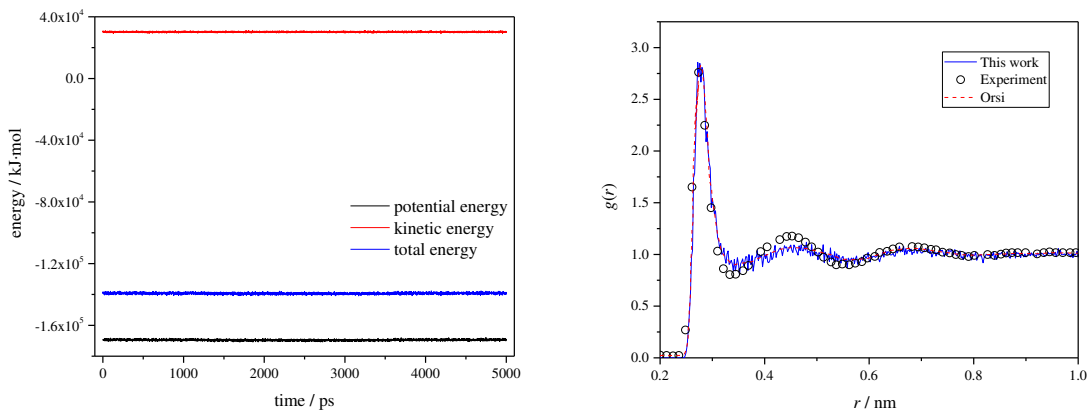
All MD simulations were conducted by GROMACS simulation package (version of 2016.03)⁷². The Gromos 53a6 force field parameters⁷³ were used to describe the properties of PAA chains, Na⁺ and Cl⁻ ions, including the potential of bonds, angles, dihedrals and non-bond interactions. The aliphatic carbon atoms with its bonded hydrogen in PAA chain were regarded as united atoms to speed up the calculations, and the Ryckaert-Bellemans (RB) potential was used for the descriptions of aliphatic torsion (CH₂-CH₁-CH₂-CH₁). The simple point charge (SPC) model was conducted to characterise water molecules. The non-bond interactions were represented by a short-range 12-6 Lennard-Jones (LJ) potential and a long range Coulombic potential, expressed in a form of pairwise interacting atomic charges. The LJ potential between two atoms can be written as follow:

$$V_{LJ}(r_{ij}) = 4\epsilon_{ij} \left[\left(\frac{\sigma_{ij}}{r_{ij}} \right)^{12} - \left(\frac{\sigma_{ij}}{r_{ij}} \right)^6 \right] \quad (1)$$

The parameters σ and ε represent energy constant and diameter of one of the atoms, which depend on atom types. The Lorentz-Berthelot combining rules were used to describe LJ potential between different atom types. The charges of atoms were adopted from previous studies^{62, 71, 74, 75}. All parameters for PAA solutions are listed in **Table S4** in the Supplement documents.

2.3 Simulation details

The leapfrog algorithm was used to integrate the motion of atoms with a time step of 2 fs. The Coulombic electrostatic interactions were calculated by using the particle Mesh Ewald (PME) method with a cut-off distance of 1.0 nm and Fourier spacing of 1.2 nm. The cut-off distance for short-range van der Waals interaction was 1.0 nm. To remove initial strain, the initial configuration was conducted by energy minimization using the Steepest Descent method. This was followed by 500 ps NVT and 500 ps NPT simulations with position restraints on PAA chains and not on water molecules to achieve a well equilibrated system. A Berendsen thermostat and a parrinello-rahman barostat were used to control the temperature and pressure at 300 K and 1 bar during the calculation with relaxation time of 0.1 ps and 0.5 ps, respectively. After full relaxation, a further 120 ns NVT simulation was performed with the water molecules fixed with SETTLE algorithm and all bonds constrained by using SHAKE procedure. The last 60 ns were conducted for the sampling and analysis. The energy variations and water distributions from the sampling period were shown in **Figure 2**, which implied a well equilibrated system and the reasonability of SPC force field for water molecules.



(a) Energy profiles

(2) Radial distribution functions of Water

Figure 2 Energy variations and water distributions in equilibrated system

3. Results and discussion

One of the efficient properties to characterise the conformation of a single polymer is the radius of gyration, R_g . In the context of these simulations, it is defined as:

$$R_g = \left(\frac{\sum_i m_i \|\mathbf{r}_i\|^2}{\sum_i m_i} \right)^{\frac{1}{2}} \quad (2)$$

Where m_i is the mass of atom i and r_i is the position of atom i with respect to the centre of mass of a PAA molecule. In this work, the radius of gyration of a fully ionized 20-monomers isotactic PAA was given a value of 1.15 nm from the last 60 ns MD simulation trajectory, which is agreed well with the previous results, as shown in **Table 1**, indicating the validation of both force field parameters and simulation protocol. The radius distribution functions (RDFs) of carboxylate, carbonyl and hydroxyl oxygen with water are also agreed well with previous work, which are shown in Figure S1 in supporting documents ⁶².

Table 1 Radius of gyration of fully ionized PAA calculated in other works

	Brownian Dynamics	Monte Carlo	Molecular simulation			Our results
Force field	coarse-grained		CHARMM 27	GROMOS 96	GROMOS 53a6	GROMOS 53a6
R_g of PAA [nm]	1.15 ⁵²	1.11 ⁵²	1.05-1.30 ⁶⁵	1.14 ⁷⁴	1.06 ⁶²	1.15

3.1 simulation size sensitivities

In this section, the effects of system size on the simulation results are discussed. With the same PAA concentration, six isotactic PAA chains with different numbers of monomers were first investigated, whose radii of gyration are shown in **Figure 3**. Similar trends are observed for all curves that as the charge density increases, the radius of gyration of the PAA chains becomes larger. The PAA chains expand rapidly with charged carboxylate groups increases ($f < 0.4$) and then slow down due to the weakening of the electrostatic repulsions caused by counter ions Na^+ ($f > 0.4$). Particularly, with the same DoI, the PAA chain with more numbers of monomers holds greater values of the radius of gyration. This is occurred even in non-ionized PAA chains, indicating that longer polymer chains tend to form larger coils in neutral state. If a shrinkage is defined as the ratio of gyrate radius of non-ionized PAA chain to fully ionized PAA chain, thereby with increasing the numbers of monomers, a reduction of the shrinkage rate is observed, indicating that the deformation of the PAA chain is more dramatic. In another word, it is much more obvious to study the conformation of a single PAA chain with more monomers.

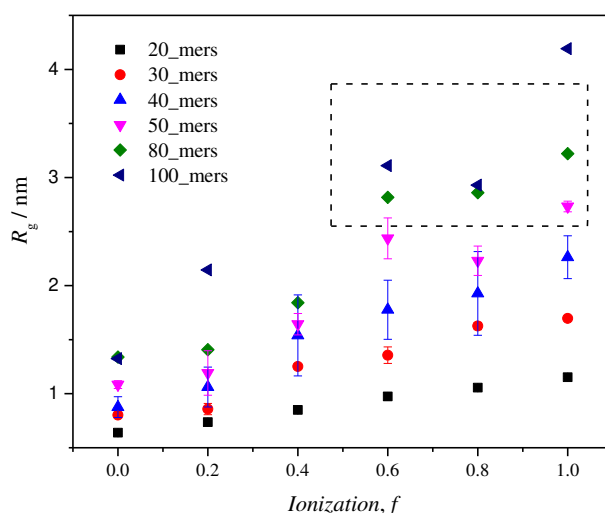


Figure 3 The averaged radius of gyration of PAA chains with different numbers of monomers

The results for PAA chains with more numbers of monomers show unexpected perturbations especially at higher DoI, which should be related to the periodicity artefacts. With a same polymer concentration, the initial and fully ionized polymer length exceed the length of the simulation box. This overlength polymer chain will be interacted with other polymer chains due to the periodic boundary conditions, which makes the polymer solutions in semi-dilute regime. Therefore, to correctly characterize behaviours of a larger oligomer in dilute state a suitable solvate volume is required. A length ratio of fully ionized PAA chains to boxes is introduced and compared in **Figure 4**. It can be observed that the length ratio is continually increasing with the increase of the numbers of monomers. As a result, when the length ratio is large enough (e.g., $L_{\text{fully}}/L_{\text{box}}=0.4$), the boxed water becomes too small for the long chain PAA to provide efficient information. Based on prior studies^{62, 65, 66, 69, 70}, a length ratio value below 0.3 was generally used and showed promising results. Further studies are conducted for 20-monomers both in large and low length ratio situations to interpret the effect of solvent volume. In addition, an enlarged simulation system with 13.4 nm for 50-monomers PAA chains also investigated as a validation.

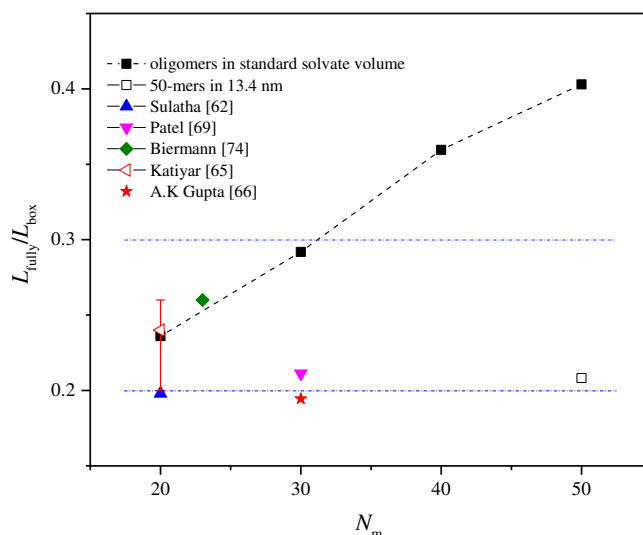
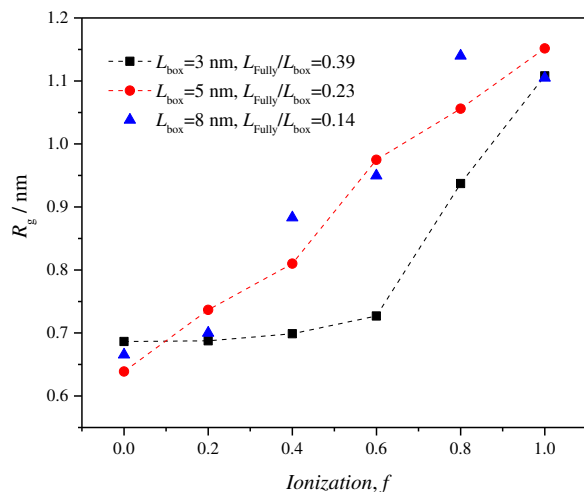
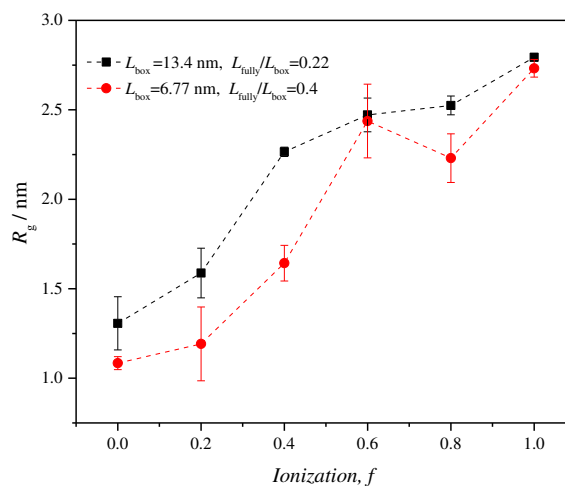


Figure 4 Variations of length ratio as a function of number of monomers

The variations of the radius of gyration in different solvent volume are plotted in **Figure 5**. When reducing the solvate volume to 3 nm with high length ratio, the behaviour of 20-monomers PAA chain in low DoI fails to be captured correctly. The R_g keeps nearly constant with the increase of DoI, which is contrast with practical conditions. In comparison with standard simulations, the enlarged solvate indeed shows good descriptions for the conformation properties of 50-monomers PAA chains. However, the corresponding calculation of such a solvate volume is time consuming and expensive. Further decrease the length ratio, same trends are obtained compared with a suitable solvent volume, which indirectly indicates that though the polymer concentration calculated in this study is as high as 1.9 wt%, it still can be regarded as a dilute solution since there is no interaction between polymer chains.



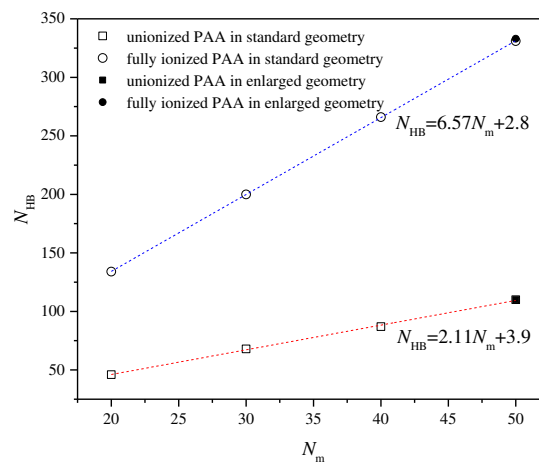
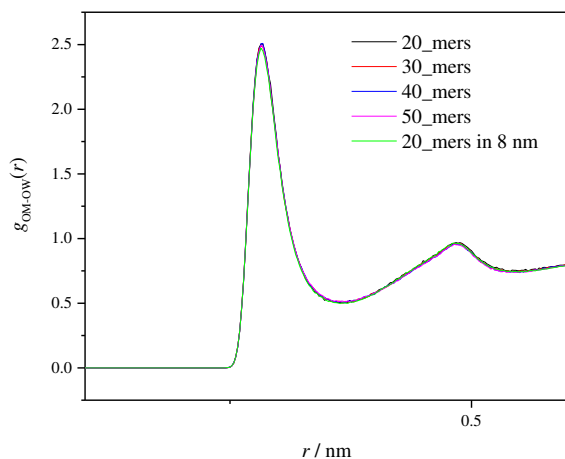
(a) 20-monomers PAA



(b) 50-monomers PAA

Figure 5 Effects of solvent volume on the radius of gyration of PAA chains

With a suitable solvent volume, the RDF profiles between PAA molecules and water as a function of the number of monomers are performed in **Figure 6(a)**. The numbers of monomers exert slightly effect on the RDFs, which indicates that neither the chain size nor the solvate volume does not affect the interaction intensity between polymer chains and water molecules. Therefore, the variations of hydrogen-bonding effect are mainly attributed to the numbers of carboxylate functional groups, which can easily be estimated from a short oligomer. The numbers of PAA-water H-bonds against different numbers of monomers PAA are calculated in **Table 2**. With increasing the numbers of monomers along the PAA chains, more H-bonds numbers are formed for both unionized PAA chains and fully ionized PAA chains. It is observed that the ionized PAA chains form about three times the number of the H-bond as that of the neutral PAA. The number of H-bonds is proportional to the chain size as the equations shown in **Figure 6(b)**. Therefore, based on the discussion mentioned above, although the longer chain exhibits much more obvious behaviours than a short chain in dilute solutions, the trends are similar, and the detailed molecular interactions are able to be inferred from a short chain polymer. This is indirectly in support of the theory that short chain polymers can represent some properties (e.g., gyrate radius) of long chain polymers in practical⁵².



(a) RDF between carboxylate groups and water (b) hydrogen bonds between PAAs and water

Figure 6 Effects of numbers of monomers on the hydration effect

Table 2 Numbers of H-bonds at different numbers of monomers

N_m	Neutral PAA	Fully ionization
20	46	134
30	68	200
40	87	266
50	110	331
50_8nm	110	333

3.1 Effect of tacticity with different degree of ionization

In this section, the effects of tacticity of different DoI are discussed since the charge along the PAA chain contributes to intramolecular repulsion theoretically and could behave variously due to the monomer associations. To reveal detailed three-dimensional information, a series of snapshots of iso-PAA at different DoI are performed in **Figure 7**. The unionized PAA chain is in a coiled state. As expected, this collapsed PAA chain gradually extends with the increase of the charge density, and finally reaches a stretched state. Same trends were found in the other two cases.

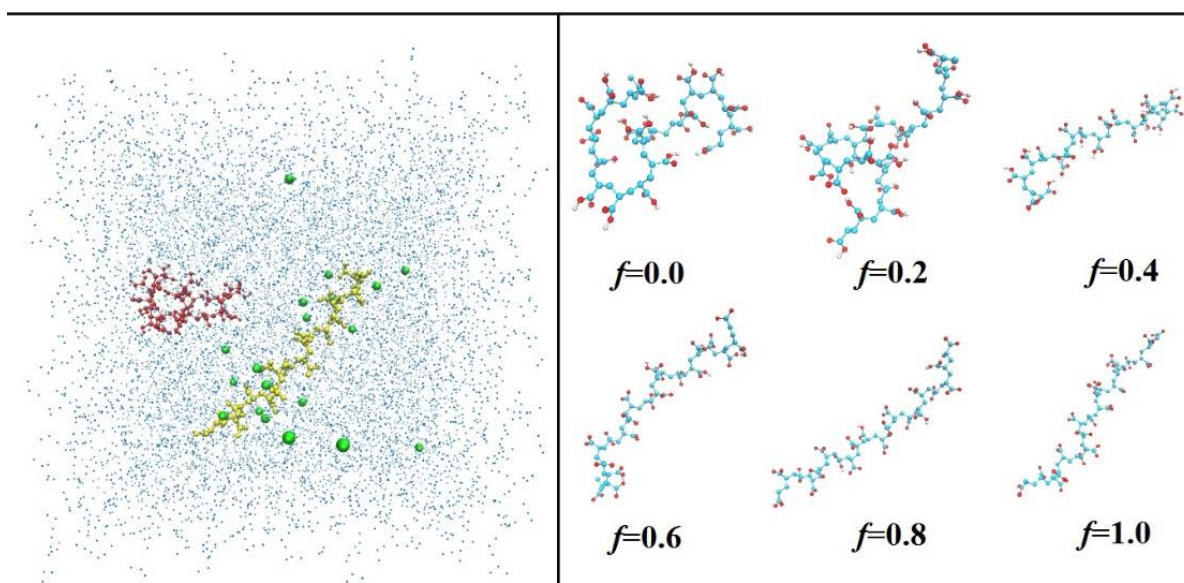
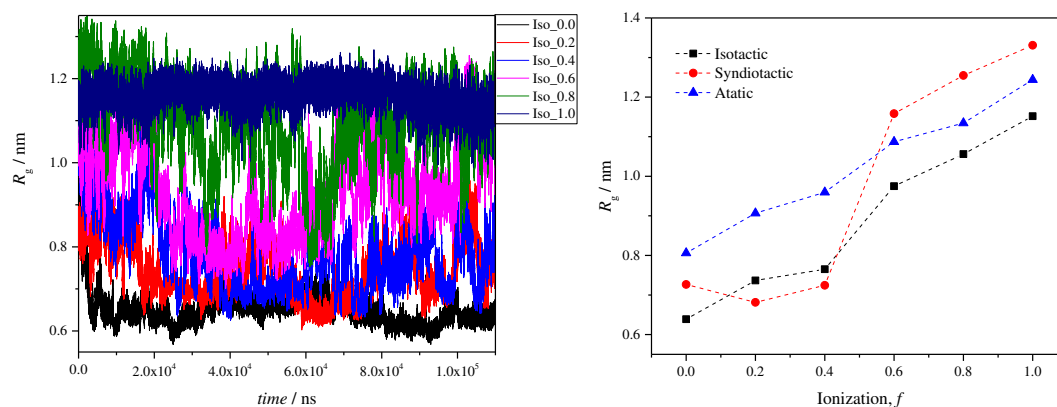


Figure 7 Snapshots of iso-PAA chains with different ionization at an equilibrated state (The left shows structure comparison of PAA chains in solutions, where the chain with red colour represents $f=0.0$, with yellow represents $f=1.0$. The green atoms represent Na^+ ions)

To quantitatively evaluate the variations of conformations of PAA chains with different DoI and tacticity, the transient and average values of R_g are plotted in **Figure 8**. The transient variations of radius of gyration show that PAA macromolecules equilibrate thermodynamically due to the Brownian motion effect. For partially ionized PAAs, these fluctuations are found to be stronger than either fully ionized or unionized PAAs, which is attributed to the random allocation of the charged COO^- groups.



(a) Instantaneous radius of gyration against time

(b) average radius of gyration

Figure 8 Variations of PAA conformation with different degrees of ionization

The average radius of gyration of 20-monomers-PAA as a function of DoI is shown in **Figure 8(b)**. Whatever tacticity of the PAA chain is, the gyrate radius continually increases from approximately 0.64 nm to 1.15 nm as the ionization increases from 0 to 1. It shows that the increased charge density cannot make the polyion to stretch itself to the fully length (compared with initial configuration) even it is totally ionized. This is because the interaction between polyion and courier-ions Na^+ would result in repression of the ionization effect, which will be discussed later. With same deprotonation patterns for these three polymer chains, the only discrepancy of the results is caused by tacticity. For the neutral case, the R_g varies with tacticity in the order atactic > syndiotactic > isotactic, which is consistent with results by A.K Gupta et al.⁷⁰. Rather than attribute to this difference to PAA initial chain configurations that adjacent COOH groups are on the opposite side of syn-PAA chain thereby holding less hydrophobic attraction than iso-PAA⁶⁵, the interpretation is performed in the **Figure 9** and described as followed. For iso-PAA, there is an interaction between monomers due to the addition of carboxylate oxygen atoms with hydroxyl hydrogen atoms in adjacent function groups. However, for syn-PAA, there exists slightly repulsion between monomers since the end of adjacent function groups are in same polarity. It is noticed that the repulsion in syndiotactic PAA is suppressed by the neighbouring repulsion as well, which weaken the stretching along the whole polymer chain. In particular, because of the random arrangement of functional groups, atactic PAA behaves both repulsions and attractions along the backbone, where the attraction strengthen the repulsion, making the polymer chain more stretched compared with syn-PAA.

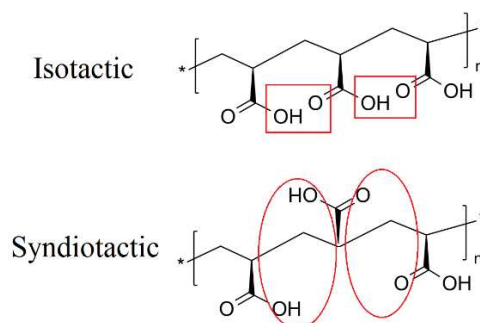


Figure 9 Tacticity effects on the polymer chain configuration, rectangular: attraction; ellipse: repulsion.

For deprotonated cases, due to the existence of sodium counter-ions, the R_g is mainly influenced by the strong electrostatic repulsions between charged groups and the shielding effects by the cations instead of the weak interaction between the neutral monomers. The effects of tacticity are dependent on DoI. At lower DoI, the R_g varies with tacticity in the order atactic > isotactic > syndiotactic while at higher DoI, an order of syndiotactic > atactic > isotactic is formed. This is because, from the RDFs shown in **Figure 13**, the syn-PAA is more attractive with Na^+ at lower DoI, which reduces the electrostatic repulsions and shrinks the polymer chain. This attraction even weakens the repulsion between the neutral monomers as well resulting in a further collapse compared with the non-ionized case. For higher DoI, however, the iso-PAA exhibits higher interaction with Na^+ than syn-PAA, which leads to a smaller R_g .

The radius distribution function (RDF) is used to investigate the interaction between PAA molecules and water as well as PAA molecules and counter-ions Na^+ , which provides further interpretation of the polymer chain formations from molecular level. The deprotonation of the carboxylic acid function groups leads to the essential differences between ionized PAA and non-ionized PAA. Therefore, the RDFs corresponding to carboxylate (COO^-) or carboxyl groups (COOH) and water molecules can provide better understanding on the effect of ionization and tacticity. Figure 10 shows the interaction for the PAA carboxylate oxygen atoms with respect to the water oxygens and hydrogens. Two peaks are founded in both RDFs profiles indicating that a double electronic layer (EDL) existed around PAA molecules. The first peaks at 0.18 nm for carboxylate oxygen atoms and water oxygen atoms, and 0.28 nm for water hydrogen atoms are similar with the hydrogen bonding distance in bulk water. These mean a strong hydrogen bonding effect dominating the interaction between carboxylate groups and water molecules. An increase of the intensity of this interaction is also observed as increased the DoI in **Figure S1(a)** in supporting documents, which demonstrates that more numbers of carboxylate groups are able to attract more water molecules. The atactic PAA shows stronger hydrophilic behaviours than the other two cases in the lower partially ionized conditions, which agreed well with the average gyrate radius trends. This discrepancy becomes insignificantly for the fully ionized PAA chains, indicating the numbers of charged groups dominates the hydration effect and the effect of tacticity of polymer can be neglected.

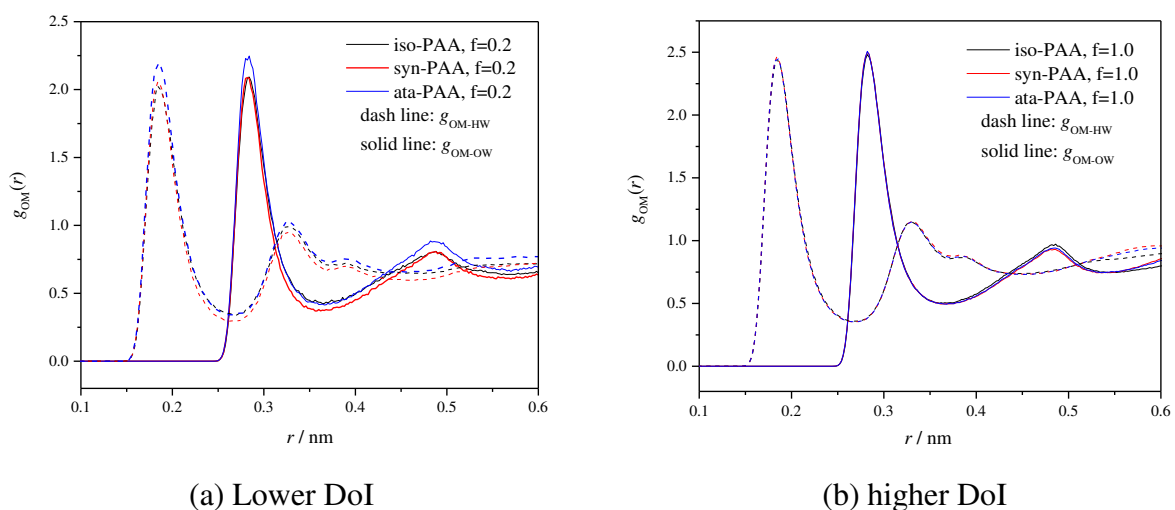
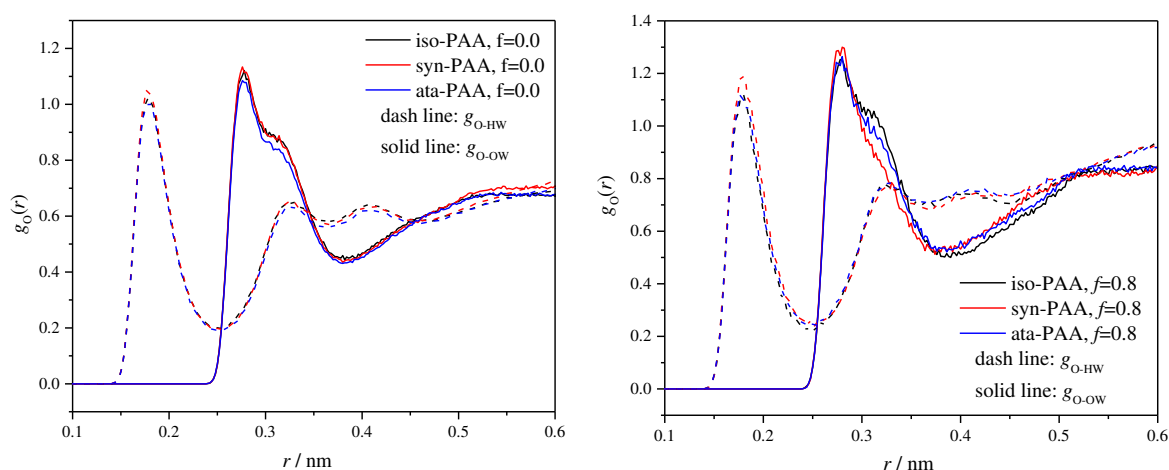


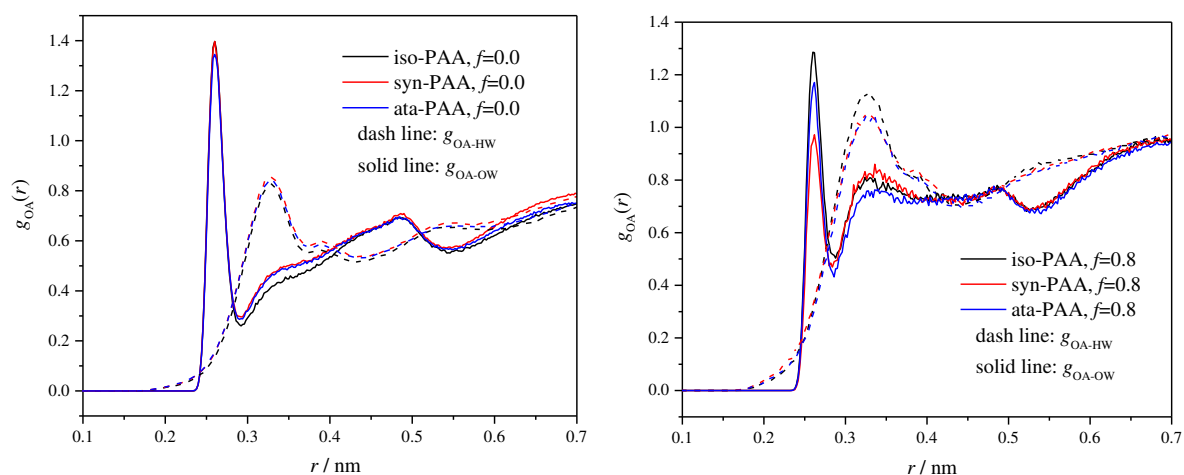
Figure 10 Radial distribution functions of carboxylate oxygen respects to water

The RDFs for the carbonyl oxygen atoms and water molecules is shown in **Figure 11**. Although the first peaks are observed at same locations with carboxylate oxygen atoms, the peak intensities are much lower. The second peaks vanish, indicating that the interaction between carbonyl oxygen atoms and water molecules are too weak to form the second water layer. In addition, there is a shoulder followed the first peak. It is interested that for neutral case, this shoulder behaviours exist independent on tacticity but for the highly ionized case, the shoulder disappears gradually as the PAA chain transform from isotactic state to syndiotactic configurations. In the case of RDFs corresponding to hydroxyl oxygen atoms and water molecules, as presented in **Figure 12**, the first peak is allocated at a slightly closer distance. However, the nearest bonding distance between hydroxyl oxygen atoms and water hydrogen atoms is approximately 0.35 nm, which shows a very weak hydrogen bonding effect between these atoms. The tacticity shows significant relationship between hydroxyl oxygens. The first peak intensity has a sharp reduction for the syndiotactic PAA compared with isotactic PAA at highly ionized conditions, indicating the hydration effect of hydroxyl oxygens in syn-PAA is the weakest. It can be concluded that due to the reduction of peak intensities and hydrogen bonding effect, the carboxylate oxygen atoms interact more intensively with water in comparison with the carbonyl oxygen and hydroxyl oxygen. Although the number of carbonyl oxygen atoms and hydroxyl oxygen atoms reduces with increasing the charge density, the increase of interaction between carboxylate oxygen and water attracts more water around PAA chain, resulting in a stronger interaction between unionized carboxyl group and water. Therefore, the trends of the ionization effect on the carbonyl oxygen and hydroxyl oxygen are similar with those of carboxylate oxygen as shown in **Figure S1** in supporting documents.



(a) Carbonyl oxygen-water at lower DoI (b) Carbonyl oxygen-water at higher DoI

Figure 11 Radial distribution functions of carbonyl oxygen respects to water



(a) Hydroxyl oxygen-water at lower DoI (b) Hydroxyl oxygen-water at higher DoI

Figure 12 Radial distribution functions of hydroxyl oxygen respects to water

The variation of the number of PAA-water H-bonds across the tacticity is studied in **Table 3**. It can be found that the number of hydrogen bond between PAA chains and water molecules increases with the increase of the charge density since the carboxylate groups attract more water than carboxyl groups. With increasing the DoI, the repulsion between intramolecular along PAA chains and the hydrogen bonding effect stretch the atoms away from the each other and attach to the water molecules, which leads to the expanding of the PAA coils and reaches a stretch state at final. Although the effects of tacticity is not significant as the electrostatic repulsion, the atactic chain forms more H-bonds compared other stereoregular chains. However, such close results demonstrate the tacticity cannot dramatically affect the hydrophilic characteristic at same ionizations, which is in contrast with the interpretation that it is the stereochemical configuration structure make the polymer chain more hydrophilic or hydrophobic to induce the discrepancy of R_g .

Table 3 Variation of H-bonds as a function of degree of ionization

tacticity	$f=0.0$	$f=0.2$	$f=0.4$	$f=0.6$	$f=0.8$	$f=1.0$
Isotactic	46.1	59.7	77.6	98.4	115.6	134.2
Syndiotactic	45.1	54.8	75.5	99.0	114.8	133.9
Atactic	47.1	63.8	73.9	95.6	109.4	132.6

The distribution of Na^+ counter ions in the vicinity of the PAA chain is represented using RDF of carboxylate oxygen atoms with respect to Na^+ ions in **Figure 13**. There are two sharp peaks: a first peak locates at 0.25 nm and a second peak locates at 0.4 nm, respectively. Although the absolute values of peaks are very high, the number of sodium ions in the near proximity are very small as described by the coordination number curves⁶⁰ in the **Figure S1(h)**. This is agreed well with the experimental fact that Na^+ are not bonded to the carboxylate groups in PAA at higher charge densities⁷⁶. From the variations of the second peak, the Na^+ ions are preferentially closer to the chain backbone, which, in return, weakens the electrostatic repulsions along the PAA chain. Therefore, in case of sodium polyacrylate, increasing ionization cannot stretch the polymer chain to its full length even at fully degree of

ionization. This counter-ions interaction with polyions varies dramatically with tacticity. For isotactic PAA chain, the intensity of the second peak strengthens with increasing the ionizations. However, these trends are not available for the syndiotactic PAA chain as the peaks along the later are almost independent on the DoI. Therefore, the interaction between polyions and counter-ions in syndiotactic case is higher than those in isotactic case at lower DoI and a reverse situation occurs at higher DoI, which as discussed above leads to different chain conformations.

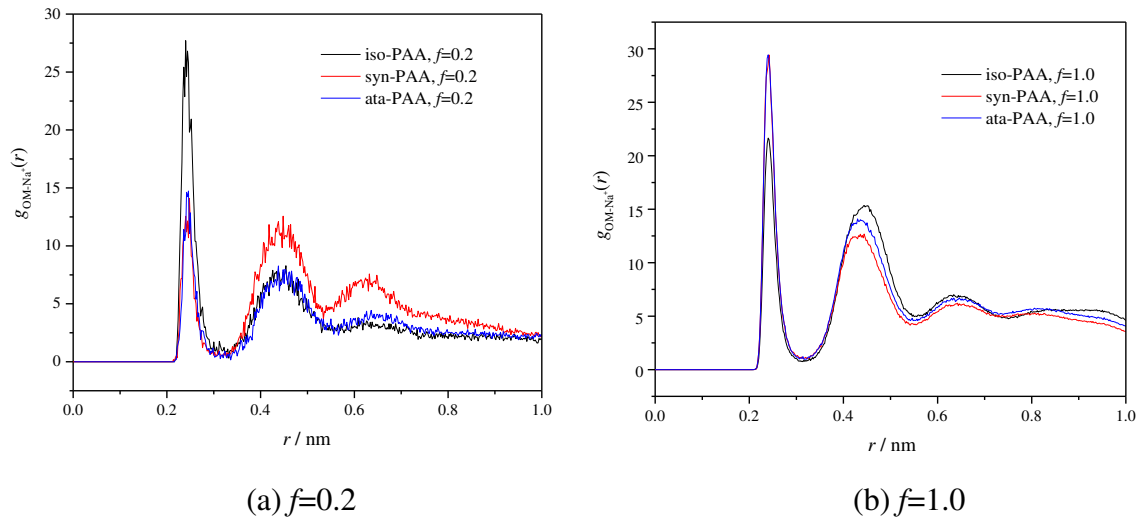


Figure 13 Radial distribution functions of PAA to counter-ions, Na^+

3.3 Effect of salinity

Based on the previous experiments and simulations, 1.5 M NaCl was regarded as a theta solvent, beyond which PAA chains are stay in unperturbed dimensions. In this study, to investigate the effect of salt, various salt concentrations ranging from 0.01 M to 1.4 M are set by inserting different numbers of sodium and chloride ions inside the simulation system, which are 0.013 M, 0.026 M, 0.066 M, 0.13 M, 0.2 M, 0.27 M, 0.66 M, and 1.33 M for 20 monomers PAA and 0 M, 0.13 M, 0.22M, 0.43 M and 0.85 M for 30 monomers PAA, respectively. The 30 monomers PAA used here is to introduce more obvious behaviours as a longer chain oligomer. The DoI for all polymer chains studied in this section was kept constant at a value of 0.4. The variations of radius of gyration along with salinity are shown in **Figure 14**.

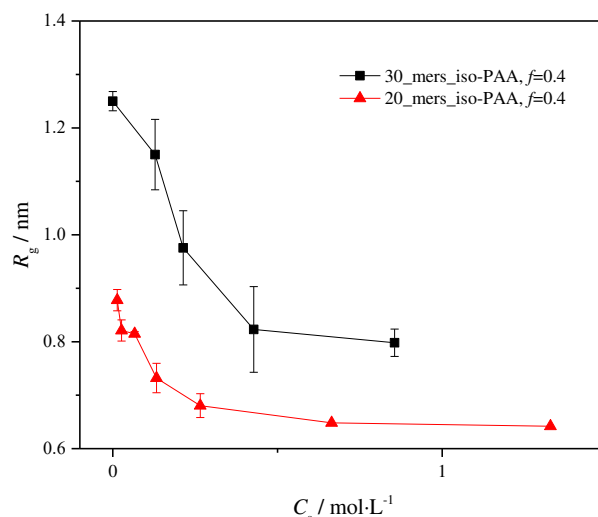


Figure 14 The variations of radius of gyration against different salinities

It can be observed that the radius of gyration of PAA chains is continually reducing with the increase of salt concentrations. There is a critical value of salinity for both curves, 0.26 for 20 monomers PAA and 0.4 for 30-monomers PAA, respectively, above which the salinity no longer affects the PAA conformation significantly. This is because the numbers of charged carboxylate groups to be shielded by salt cations are limited. In addition, the longer PAA chain (30-monomers) is more sensitive with salinity than the shorter PAA chain (20-monomers). As discussed from the previous section, increasing the number of monomers is beneficial to investigate the conformation properties. Due to the additional number of charged carboxylate groups, the shielding effect is more significant.

30-monomers-PAA:

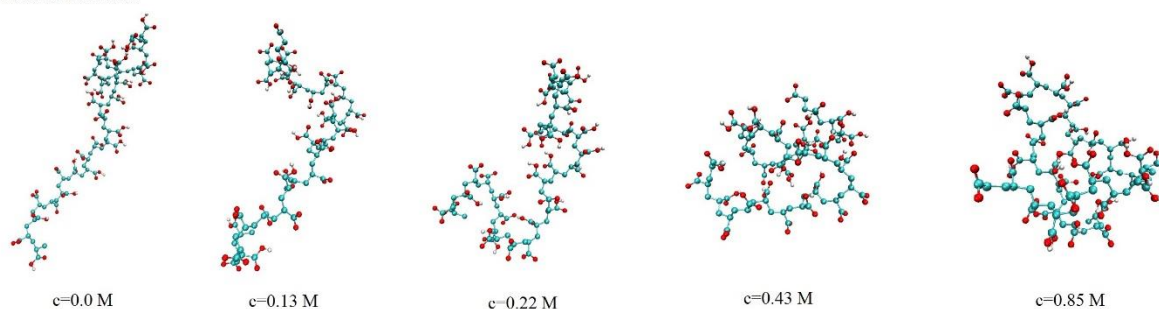


Figure 15 Series of snapshots of PAA structure against different salinities

The equilibrated configuration snapshots of 30 monomers PAA chain after 120 ns simulation period are presented in **Figure 15**. With increasing the salt concentration, the PAA chains collapse gradually. In particular, for the 30-monomers PAA chain, a coil-like conformation is formed by shielding effect when salt concentration reaches the critical value.

The effects of tacticity in the presence of salt are investigated as well for 20 monomers PAA chains under similar salinity range. The variations of average R_g as a function of salinity are performed in **Figure 16**. For all the three cases, the gyrate radius of polymer chains reduces with increasing the salinity. However, at lower salt concentrations, the syn-PAA is more collapsed than iso-PAA. This is attributed to the random deprotonation patterns. As shown in **Figure 17**, there is a cluster of charged carboxylate groups along the mid of the polymer

chain. For iso-PAA, the distance between carboxylate function groups are much closer than those in syn-PAA, which makes the polymer chains form a rod-like structure. Unlike the iso-PAA, the syn-PAA chain forms a sphere-like structures due to the cations shielding effects. These different structures lead to different gyrate radius. However, as the salinity increases, the repulsion along the iso-PAA chain is also suppressed, resulting similar conformations for both chains.

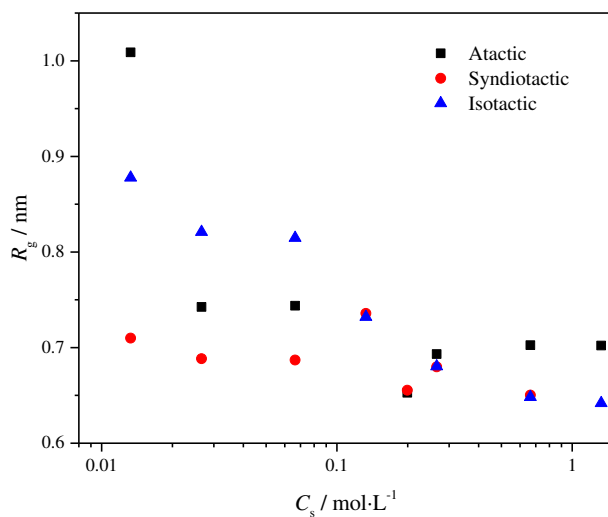


Figure 16 Tacticity effects on the radius of gyration in the presence of salt

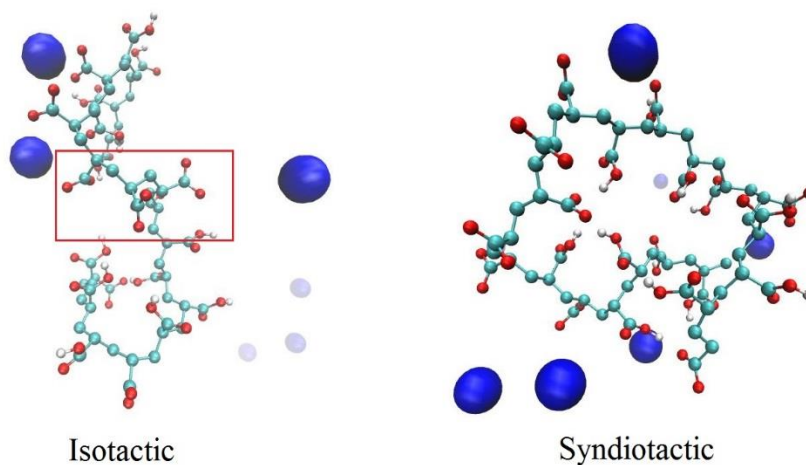
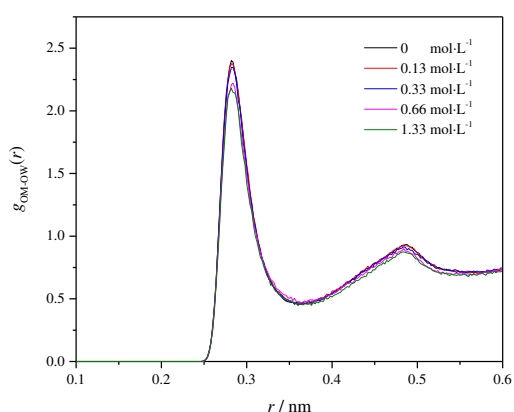
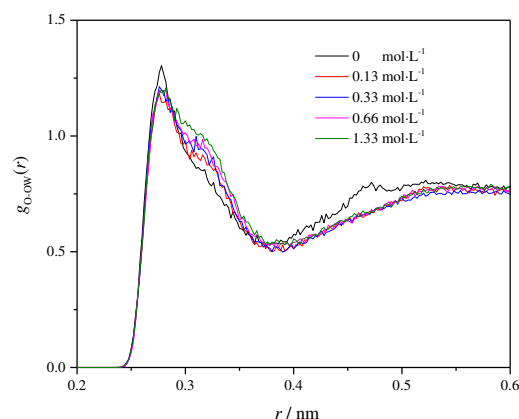


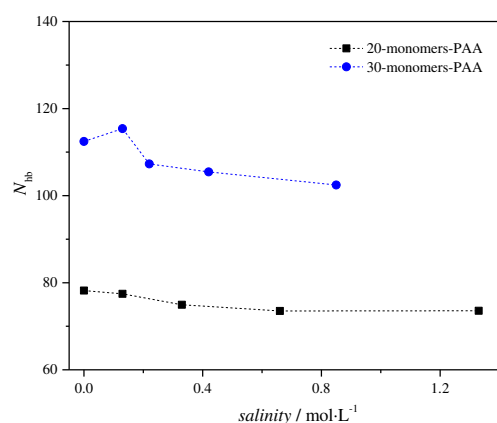
Figure17 Snapshots of isotactic and syndiotactic chains at salinity value of 0.026 M, (cyan: PAA backbone; blue Na^+ ; Cl^- is not shown)



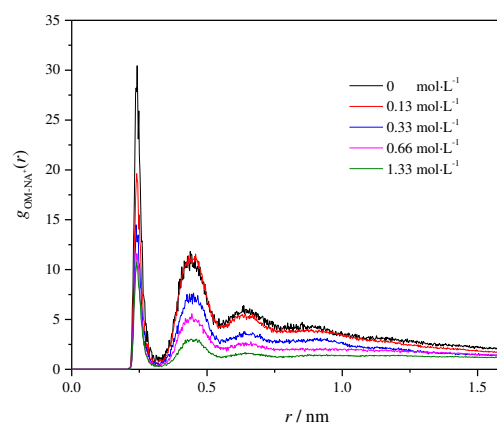
(a) Carboxylate oxygen-water oxygen pairs



(b) Carbonyl oxygen-water oxygen pairs



(c) Hydroxyl oxygen-water oxygen pairs



(d) Carboxylate oxygen-sodium ions pairs

Figure 18 RDFs and hydration effects between PAA and water as a function of salinity

The RDF profiles between PAA molecules and water under different salinities are shown in **Figure 18** to reveal the further effects of salinity. The PAA chains with 30 monomers are selected as a representation since the number of monomers does not influence the atomic interaction intensities. It can be found that the increase of salinity can indeed weaken the interaction between carboxylate oxygen atoms and water oxygen atoms in **Figure 18(a)**, which consequently diminish the hydrogen bonding effect. Besides, the first sharp peak of $g_{O_{H_2O}}(r)$ in **Figure 18(b)** tends to be a broad shoulder and the peak intensity decreases at higher salinity. These indicate that the water prefers to diffuse into the bulk and less water is attached to PAA macro molecules. However, the salinity effect on hydrogen interaction is not dramatic as the number of H-bonds between water and PAA chains changes not significantly. **Figure 18(c)** performs the number of H-bonds formed under different salt concentrations. The values of H-bonds slightly vary from 111 to 102 and 78 to 74 for 30-monomers PAA and 20-monomers PAA, respectively. Therefore, it can be inferred that the salinity changes the PAA chain conformation mainly by pure electrostatic interactions between PAA chains and salt ions rather than the hydrogen bonding effects of PAA chains respected to water molecules. The electrostatic interactions also called shielding effect or electrostatic screening effect increases with the increase of salt concentrations, which in return, causes a reduction in the attractive interactions between PAA chains and salt ions, represented by a decrease of peak intensity in **Figure 18(d)**.

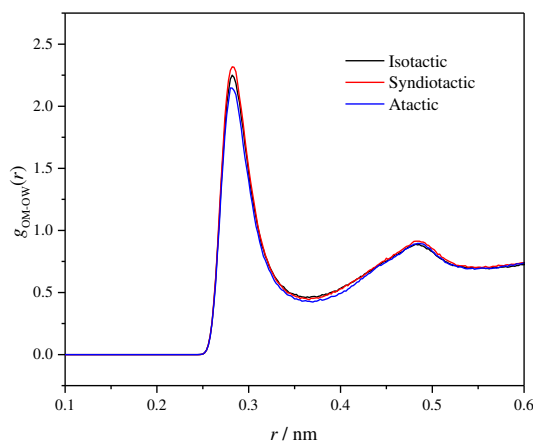


Figure 19 The effect of tacticity on hydration interaction at the value of salinity 0.26 M

The discrepancy of hydration interaction based on tacticity is performed in **Figure 19** by the RDF curves between carboxylate oxygens and water molecules. The syn-PAA has a much stronger interaction with water in the presence of salt. As a result, the syn-PAA is much easier to be dissolved into NaCl aqueous solution. It should be noted that it is the electrostatic repulsion and the counter-ions shielding effect that dominates the polymer behaviours in stock salt solutions rather than this hydrophilic characteristic

4. Conclusion

The conformational and hydration behaviour of a single polyacrylic acid (PAA) chain in dilute solutions as a function of degree of ionization with different chain size, solvent volume, tacticity and salt concentrations were investigated by atomistic molecular dynamics simulations with explicit solvate and ions description. The main simulation results can be concluded as below:

A suitable solvent volume is required for a certain polymer chain to achieve a dilute situation, otherwise, the behaviours are not able to be captured correctly based on the interactions between polymer chains. The number of monomers does not affect the intensity of the hydration between PAA chains and water molecules. The hydrogen bonding effect could be estimated from shorter oligomers. Although long chain polymer tends to have a more dramatically deformation, this behaviour could be observed in a short as well.

The tacticity does affect the PAA configurations both in salt free and salt conditions. In the salt free solutions, the gyrate radius of the syndiotactic PAA is larger than isotactic PAA both in neutral state and fully ionized state. The former is mainly attributed to the repulsion between adjacent monomers along the PAA chain and the latter is due to the weak interaction between counter-ions. Whatever the PAA chain is, the gyrate radius reduces with the salinity increasing. This is because the strong shielding effects rather than the hydrophilic characteristic. The isotactic used in this study forms a rob-like structure due to repulsion between neighbouring carboxylate function groups, while the syndiotactic PAA is in a sphere-like structure. This discrepancy disappears when the salinity reaches a high degree and similar conformations are obtained for PAA chains with different tacticity.

ASSOCIATED CONTENT

Supporting information. Detailed information for 20 monomers isotactic, syndiotactic, and atactic polymer (**Table S1-S4**); RDFs for 20-iso PAA as a function of DoI

AUTHOR INFORMATION

Corresponding Author

Emails: d.wen@buaa.edu.cn

FUNDING SOURCES

This work was supported by European research council consolidator grant (grant number: 648375) and China scholarship council (Mr G. Yao and Ms. J Zhao)

REFERENCES

1. Kuo, A. C. Poly (dimethylsiloxane). *Polymer data handbook*; Mark, J. E.; Oxford university press: New York, 1999; pp 411-435.
2. Jiang, H.; Taranekar, P.; Reynolds, J. R.; Schanze, K. S. Conjugated polyelectrolytes: synthesis, photophysics, and applications. *Angew. Chem., Int. Ed.* **2009**, *48* (24), 4300-4316.
3. Peyratout, C. S.; Daehne, L. Tailor-made polyelectrolyte microcapsules: from multilayers to smart containers. *Angew. Chem., Int. Ed.* **2004**, *43* (29), 3762-3783.
4. Schmaljohann, D. Thermo-and pH-responsive polymers in drug delivery. *Adv. Drug Delivery Rev.* **2006**, *58* (15), 1655-1670.
5. Zhong, C.; Luo, P.; Ye, Z.; Chen, H. Characterization and solution properties of a novel water-soluble terpolymer for enhanced oil recovery. *Polym. Bull.* **2009**, *62* (1), 79-89.
6. Muller, G.; Laine, J.; Fenyó, J. High-molecular-weight hydrolyzed polyacrylamides. I. Characterization. Effect of salts on the conformational properties. *J. Polym. Sci., Part A: Polym. Chem.* **1979**, *17* (3), 659-672.
7. Papkov, S.; Kulichikhin, V.; Kalmykova, V.; Malkin, A. Y. Rheological properties of anisotropic poly (para-benzamide) solutions. *J. Polym. Sci., Part B: Polym. Phys.* **1974**, *12* (9), 1753-1770.
8. Choi, J.; Rubner, M. F. Influence of the degree of ionization on weak polyelectrolyte multilayer assembly. *Macromolecules* **2005**, *38* (1), 116-124.
9. Markovitz, H.; Kimball, G. E. The effect of salts on the viscosity of solutions of polyacrylic acid. *J. Colloid Sci.* **1950**, *5* (2), 115-139.
10. Choi, S. K. pH sensitive polymers for novel conformance control and polymer flooding applications. Ph.D. Thesis, The University of Texas at Austin, 2008.
11. Krasny-Ergen, W. Untersuchungen über die viskosität von suspensionen und lösungen. 2. zur theorie der elektroviskosität. *Kolloid-Z.* **1936**, *74* (2), 172-178.
12. Katchalsky, A.; Spitnik, P. Potentiometric titrations of polymethacrylic acid. *J. Polym. Sci., Part A: Polym. Chem.* **1947**, *2* (4), 432-446.
13. Staudinger, H. *Die hochmolekularen organischen Verbindungen: Kautschuk und Cellulose*; Springer-Verlag: Berlin, 2013.
14. Bhargava, H.; Srivastava, R. R.; Singh, M. Viscosities of Copolyphosphates in Salt-Free Aqueous Solutions and Theta Solvents I. *Polym. J.* **1987**, *19* (11), 1285.

15. Eisenberg, H. Polyelectrolyte excluded volume and expansion compared to non-ionic polymers. *Acta Polym.* **1998**, *49* (10-11), 534-538.
16. Delcroix, M.; Demoustier-Champagne, S.; Dupont-Gillain, C. C. Quartz crystal microbalance study of ionic strength and pH-dependent polymer conformation and protein adsorption/desorption on PAA, PEO, and mixed PEO/PAA brushes. *Langmuir* **2013**, *30* (1), 268-277.
17. Fan, A.; Turro, N. J.; Somasundaran, P. A study of dual polymer flocculation. *Colloids Surf., A* **2000**, *162* (1-3), 141-148.
18. Pan, Z.; Campbell, A.; Somasundaran, P. Polyacrylic acid adsorption and conformation in concentrated alumina suspensions. *Colloids Surf., A* **2001**, *191* (1-2), 71-78.
19. Kim, Y.-H.; Lee, S.-M.; Lee, K.-J.; Paik, U.; Park, J.-G. Constraints on removal of Si₃N₄ film with conformation-controlled poly (acrylic acid) in shallow-trench isolation chemical-mechanical planarization (STI CMP). *J. Mater. Res.* **2008**, *23* (1), 49-54.
20. Dong, R. Y.; Tomchuk, E.; Wade, C. G.; Visintainer, J.; Bock, E. Deuteron line shape study of molecular order and conformation in the nematogens PAA and MBBA. *J. Chem. Phys.* **1977**, *66* (9), 4121-4125.
21. Dianoux, A.; Ferreira, J.; Martins, A.; Giroud, A.; Volino, F. Molecular Structure, Conformation and Orientational Order of Para-Azoxy-Anisole (PAA) in the Nematic Phase, and Their Temperature Dependence: Results from a Deuterium and Proton Magnetic Resonance Study. *Mol. Cryst. Liq. Cryst.* **1985**, *116* (3-4), 319-352.
22. Hara, M.; Nakajima, A. Characteristic behaviors of light scattering from polyelectrolyte in dilute solution region. *Polym. J.* **1980**, *12* (10), 701.
23. Noda, I.; Imai, M.; Kitano, T.; Nagasawa, M. Particle scattering factor of polymer chains with excluded volumes. *Macromolecules* **1983**, *16* (3), 425-428.
24. Schweins, R.; Hollmann, J.; Huber, K. Dilute solution behaviour of sodium polyacrylate chains in aqueous NaCl solutions. *Polymer* **2003**, *44* (23), 7131-7141.
25. Schweins, R.; Huber, K. Collapse of sodium polyacrylate chains in calcium salt solutions. *Eur. Phys. J. E* **2001**, *5* (1), 117-126.
26. Schweins, R.; Lindner, P.; Huber, K. Calcium induced shrinking of NaPA chains: A SANS investigation of single chain behavior. *Macromolecules* **2003**, *36* (25), 9564-9573.
27. Wu, C.; Chan, K. K.; Xia, K.-Q. Experimental study of the spectral distribution of the light scattered from flexible macromolecules in very dilute solution. *Macromolecules* **1995**, *28* (4), 1032-1037.
28. Pohlmeier, A.; Haber-Pohlmeier, S. Ionization of short polymethacrylic acid: titration, DLS, and model calculations. *J. Colloid Interface Sci.* **2004**, *273* (2), 369-380.
29. Satoh, K.; Kuroki, S.; Satoh, M. Charge density-dependent coil-globule transition of alkali metal polycarboxylates in aqueous organic solvent mixtures. *Colloid Polym. Sci.* **2013**, *291* (6), 1453-1462.
30. Takani, S.; Satoh, M. Temperature-induced coil-globule transition of alkali metal polyacrylates in aqueous organic solvent mixtures. *J. Macromol. Sci., Part B: Phys.* **2016**, *55* (9), 955-967.
31. Borochoy, N.; Eisenberg, H. Stiff (DNA) and flexible (NaPSS) polyelectrolyte chain expansion at very low salt concentration. *Macromolecules* **1994**, *27* (6), 1440-1445.
32. Flory, P. J.; Osterheld, J. E. Intrinsic viscosities of polyelectrolytes. poly-(acrylic acid). *J. Phys. Chem.* **1954**, *58* (8), 653-661.
33. Takahashi, A.; Nagasawa, M. Excluded volume of polyelectrolyte in salt solutions. *J. Am. Chem. Soc.* **1964**, *86* (4), 543-548.
34. Peterlin, A. Excluded volume effect on light scattering of the coiled linear macromolecule. *J. Chem. Phys.* **1955**, *23* (12), 2464-2465.
35. Kratky, O.; Porod, G. *Rec. trav. chim.* **1949**, *68*, 1106.
36. Ikegami, A.; Imai, N. Precipitation of polyelectrolytes by salts. *J. Polym. Sci.* **1962**, *56* (163), 133-152.
37. Huber, K. Calcium-induced shrinking of polyacrylate chains in aqueous solution. *J. Phys. Chem.* **1993**, *97* (38), 9825-9830.
38. Muthukumar, M. Theory of counter-ion condensation on flexible polyelectrolytes: adsorption mechanism. *J. Chem. Phys.* **2004**, *120* (19), 9343-9350.

39. Wang, Q.; Taniguchi, T.; Fredrickson, G. H. Self-consistent field theory of polyelectrolyte systems. *J. Phys. Chem. B* **2004**, *108* (21), 6733-6744.
40. Wang, H.; Zhang, H.; Liu, C.; Yuan, S. Coarse-grained molecular dynamics simulation of self-assembly of polyacrylamide and sodium dodecylsulfate in aqueous solution. *J. Colloid Interface Sci.* **2012**, *386* (1), 205-211.
41. Shang, B. Z.; Wang, Z.; Larson, R. G. Molecular dynamics simulation of interactions between a sodium dodecyl sulfate micelle and a poly (ethylene oxide) polymer. *J. Phys. Chem. B* **2008**, *112* (10), 2888-2900.
42. Cao, Q.; Zuo, C.; Li, L.; He, H. Self-assembled nanostructures of bottle-brush polyelectrolytes with oppositely charged surfactants: a computational simulation study. *Soft Matter* **2011**, *7* (14), 6522-6528.
43. Yuan, S.-M.; Yan, H.; Lv, K.; Liu, C.-B.; Yuan, S.-L. Surface behavior of a model surfactant: A theoretical simulation study. *J. Colloid Interface Sci.* **2010**, *348* (1), 159-166.
44. Zhang, J.; Borg, M. K.; Ritos, K.; Reese, J. M. Electrowetting controls the deposit patterns of evaporated salt water nanodroplets. *Langmuir* **2016**, *32* (6), 1542-1549.
45. Zhang, J.; Borg, M. K.; Sefiane, K.; Reese, J. M. Wetting and evaporation of salt-water nanodroplets: A molecular dynamics investigation. *Phys. Rev. E* **2015**, *92* (5), 052403.
46. Uchida, H.; Matsuoka, M. Molecular dynamics simulation of solution structure and dynamics of aqueous sodium chloride solutions from dilute to supersaturated concentration. *Fluid Phase Equilib.* **2004**, *219* (1), 49-54.
47. Patra, M.; Karttunen, M. Systematic comparison of force fields for microscopic simulations of NaCl in aqueous solutions: diffusion, free energy of hydration, and structural properties. *J. Comput. Chem.* **2004**, *25* (5), 678-689.
48. Chowdhuri, S.; Chandra, A. Molecular dynamics simulations of aqueous NaCl and KCl solutions: Effects of ion concentration on the single-particle, pair, and collective dynamical properties of ions and water molecules. *J. Chem. Phys.* **2001**, *115* (8), 3732-3741.
49. Driesner, T.; Seward, T.; Tironi, I. Molecular dynamics simulation study of ionic hydration and ion association in dilute and 1 molal aqueous sodium chloride solutions from ambient to supercritical conditions. *Geochim. Cosmochim. Acta* **1998**, *62* (18), 3095-3107.
50. Lyubartsev, A. P.; Laaksonen, A. Concentration effects in aqueous NaCl solutions. A molecular dynamics simulation. *J. Phys. Chem.* **1996**, *100* (40), 16410-16418.
51. Zhu, S. B.; Robinson, G. W. Molecular-dynamics computer simulation of an aqueous NaCl solution: Structure. *J. Chem. Phys.* **1992**, *97* (6), 4336-4348.
52. Reith, D.; Müller, B.; Müller-Plathe, F.; Wiegand, S. How does the chain extension of poly (acrylic acid) scale in aqueous solution? A combined study with light scattering and computer simulation. *J. Chem. Phys.* **2002**, *116* (20), 9100-9106.
53. Laguerre, A.; Ulrich, S.; Labille, J.; Fatin-Rouge, N.; Stoll, S.; Buffle, J. Size and pH effect on electrical and conformational behavior of poly (acrylic acid): simulation and experiment. *Eur. Polym. J.* **2006**, *42* (5), 1135-1144.
54. Pantano, D. A.; Klein, M. L.; Discher, D. E.; Moore, P. B. Morphologies of charged diblock copolymers simulated with a neutral coarse-grained model. *J. Phys. Chem. B* **2011**, *115* (16), 4689-4695.
55. Mantha, S.; Yethiraj, A. Conformational properties of sodium polystyrenesulfonate in water: Insights from a coarse-grained model with explicit solvent. *J. Phys. Chem. B* **2015**, *119* (34), 11010-11018.
56. Carrillo, J.-M. Y.; Dobrynin, A. V. Salt effect on osmotic pressure of polyelectrolyte solutions: simulation study. *Polymers* **2014**, *6* (7), 1897-1913.
57. Dimitrov, D.; Milchev, A.; Binder, K. Polymer brushes in solvents of variable quality: Molecular dynamics simulations using explicit solvent. *J. Chem. Phys.* **2007**, *127* (8), 084905.
58. Limbach, H. J.; Holm, C. Single-chain properties of polyelectrolytes in poor solvent. *J. Phys. Chem. B* **2003**, *107* (32), 8041-8055.
59. Zhou, Z.; Davis, P. J. Molecular dynamics study of polymer conformation as a function of concentration and solvent quality. *J. Chem. Phys.* **2009**, *130* (22), 224904.

60. Ramachandran, S.; Katha, A. R.; Kolake, S. M.; Jung, B.; Han, S. Dynamics of dilute solutions of poly (aspartic acid) and its sodium salt elucidated from atomistic molecular dynamics simulations with explicit water. *J. Phys. Chem. B* **2013**, *117* (44), 13906-13913.
61. Sitar, S.; Aseyev, V.; Kogej, K. Differences in association behavior of isotactic and atactic poly (methacrylic acid). *Polymer* **2014**, *55* (3), 848-854.
62. Sulatha, M. S.; Natarajan, U. Origin of the difference in structural behavior of poly (acrylic acid) and poly (methacrylic acid) in aqueous solution discerned by explicit-solvent explicit-ion MD simulations. *Ind. Eng. Chem. Res.* **2011**, *50* (21), 11785-11796.
63. Sulatha, M. S.; Natarajan, U. Molecular dynamics simulations of PAA–PMA polyelectrolyte copolymers in dilute aqueous solution: chain conformations and hydration properties. *Ind. Eng. Chem. Res.* **2012**, *51* (33), 10833-10839.
64. Sappidi, P.; Natarajan, U. Polyelectrolyte conformational transition in aqueous solvent mixture influenced by hydrophobic interactions and hydrogen bonding effects: PAA–water–ethanol. *J. Mol. Graphics Modell.* **2016**, *64*, 60-74.
65. Katiyar, R. S.; Jha, P. K. Phase behavior of aqueous polyacrylic acid solutions using atomistic molecular dynamics simulations of model oligomers. *Polymer* **2017**, *114*, 266-276.
66. Gupta, A. K.; Natarajan, U. Anionic polyelectrolyte poly (acrylic acid)(PAA) chain shrinkage in water–ethanol solution in presence of Li⁺ and Cs⁺ metal ions studied by molecular dynamics simulations. *Mol. Simul.* **2017**, *43* (8), 625-637.
67. Buló, R. E.; Donadio, D.; Laio, A.; Molnar, F.; Rieger, J.; Parrinello, M. “Site Binding” of Ca²⁺ Ions to Polyacrylates in Water: A Molecular Dynamics Study of Coiling and Aggregation. *Macromolecules* **2007**, *40* (9), 3437-3442.
68. Molnar, F.; Rieger, J. “Like-charge attraction” between anionic polyelectrolytes: molecular dynamics simulations. *Langmuir* **2005**, *21* (2), 786-789.
69. Patel, K. H.; Chockalingam, R.; Natarajan, U. Molecular dynamic simulations study of the effect of salt valency on structure and thermodynamic solvation behaviour of anionic polyacrylate PAA in aqueous solutions. *Mol. Simul.* **2017**, *43* (9), 691-705.
70. Gupta, A. K.; Natarajan, U. Tacticity effects on conformational structure and hydration of poly-(methacrylic acid) in aqueous solutions-a molecular dynamics simulation study. *Mol. Simul.* **2016**, *42* (9), 725-736.
71. Hoda, N.; Larson, R. G. Explicit-and implicit-solvent molecular dynamics simulations of complex formation between polycations and polyanions. *Macromolecules* **2009**, *42* (22), 8851-8863.
72. Hess, B.; Kutzner, C.; Van Der Spoel, D.; Lindahl, E. GROMACS 4: algorithms for highly efficient, load-balanced, and scalable molecular simulation. *J. Chem. Theory Comput.* **2008**, *4* (3), 435-447.
73. Oostenbrink, C.; Villa, A.; Mark, A. E.; Van Gunsteren, W. F. A biomolecular force field based on the free enthalpy of hydration and solvation: the GROMOS force-field parameter sets 53A5 and 53A6. *J. Comput. Chem.* **2004**, *25* (13), 1656-1676.
74. Biermann, O.; Hädicke, E.; Koltzenburg, S.; Seufert, M.; Müller-Plathe, F. Hydration of polyelectrolytes studied by molecular dynamics simulation, **2001**. Cornell University library. <https://arxiv.org/abs/cond-mat/0101115> (accessed Oct 25, 2018).
75. Oldiges, C.; Tönsing, T. Molecular dynamic simulation of structural, mobility effects between dilute aqueous CH₃CN solution and crosslinked PAA Part 1. Structure. *Phys. Chem. Chem. Phys.* **2002**, *4* (9), 1628-1636.
76. Koda, S.; Nomura, H.; Nagasawa, M. Raman spectroscopic studies on the interaction between counterion and polyion. *Biophys. Chem.* **1982**, *15* (1), 65-72.

Table of Contents Graphic

